IEEE Access
Multidisciplinary | Rapid Review | Open Access Journal

Received July 7, 2019, accepted July 21, 2019, date of publication July 23, 2019, date of current version August 9, 2019.

Digital Object Identifier 10.1109/ACCESS.2019.2930660

Lightweight, High Performance Detection Method of Pipeline Defects Through Compact Off-Axis Magnetization and Sensing

LI JIAN, GE YU, AND HUANG XINJING

State Key Laboratory of Precision Measuring Technology and Instruments, Tianjin University, Tianjin 300072, China
Binhai International Advanced Structural Integrity Research Centre, Tianjin 300072, China

Corresponding author: Huang Xinjing (huangxinjing@tju.edu.cn)

This work was supported in part by the National Natural Science Foundation of China under Grant 61773283 and Grant 51604192, and in part by the Project funded by the China Postdoctoral Science Foundation under Grant 2018M630271.

ABSTRACT This paper proposes a new lightweight, low cost, and high performance detection method of pipeline defects through compact off-axis magnetization and sensing. By deploying the magnetic sensor below the edge of the tiny magnet instead of its center, high magnetic sensitivity of defect detection can be achieved while magnetic sensing saturation can be avoided. It is experimentally demonstrated that both the sensitivity and effective lift-off value of defect detections are significantly enhanced. For various defects of different sizes and shapes, the sensitivity of the proposed scheme is mostly enhanced by 2–12 times and sometimes up to 20 times, compared with passive magnetic detection; the effective lift-off values are as high as 6 mm–13 mm, which exceeds conventional magnetic detection methods and is also much larger than the thickness of the protective polyurethane layer on the probe required by a field pipeline detector. In addition, speed independence as for the detected magnetic characteristics makes the proposed probe particularly suitable for the pipeline detector whose moving speed is unstable. Finally, its capacity of detecting a real oil-stealing hole is experimentally demonstrated.

INDEX TERMS Pipeline, magnetic field, defect detection, magnetization.

I. INTRODUCTION

Steel pipelines are the most important infrastructure for transporting oil and natural gas. Security issues are one important aspect of pipeline operation management. Over time, a pipeline will deteriorate with its integrity destroyed in the defect forms of pits, cracks, scratches, and holes due to electrochemical corrosion, inflow erosion, drilling by thieves for stealing oil [1]–[3]. As the defects develop, the pipeline may fracture and leaked oil/gas will result in direct economic loss, personal injury and death, severe environmental pollution, and costly pipeline repair and environment restoration.

There are many non-destructive testing (NDT) methods that can be employed for detecting and locating the pipeline defects [4]–[6], such as magnetic flux leakage testing (MFLT), ultrasonic testing (UT), eddy current testing (ECT), and permanent magnet perturbation (PMP) testing. As the long pipelines are buried underground and their transportation tasks cannot be interrupted long periods of time, the above NDT methods must be implemented via smart online in-pipe inspection tools (Pipeline Inspection Gauges, PIGs) [7], [8]. Each NDT method based on a PIG has its advantages but also limitations.

MFLT has become the most important inspection method because it is sensitive to various sharp type defects and valid for both external and internal defects [5], [6]. It thoroughly magnetizes the pipe wall along the pipe axial direction until the magnetic saturation point is reached. Magnetic flux leaking over metal loss defects are picked up to infer the change in volume of metal near a defect. Because the power consumption and weight of the magnetizer is very large, the PIG equipped with MFLT devices is very huge and cumbersome. UT sends straight ultrasonic beams at discrete intervals throughout the pipe wall and record the echoes to estimate the pipeline wall thickness [1], [4]. It requires couplant, so a UT PIG can only run in a liquid filled pipeline. It works well with heavy-wall pipe, but not as well as with thin wall pipe. ECT is based on an interruption in the secondary

The associate editor coordinating the review of this manuscript and approving it for publication was Kai Li.

magnetic field of an eddy current by a flaw in a tested object [1], [4], [9]. ECT can quickly and sensitively detect tight cracks without the use of couplant, but requires a very small liftoff value to maintain a sufficient sensitivity that is likely to be lowered due to the coating on the pipe inwall and the protective layer on the probe.

Both high power excitation device and complex signal conditioning module are required by MFLT, UT, and ECT, so the PIG is very huge in size, weight, and power consumption, usually being implemented once every 2-4 years. If a more compact and lightweight defect detection method is developed, PIG-based inspection can be more frequently carried out to achieve quasi-real-time pipeline scans and multiple acquisitions. Quasi-real-time inspection is very important to safe pipeline operations. For example, it can in time detect the oil-stealing hole (OSH) which is a very common and great threat to the pipelines.

Weak magnetic detection is not only applied for non-ferromagnetic materials such as aluminium and crystal silicon, but also applied for ferromagnetic pipe, as long as the magnetization is much smaller than the saturation magnetization, as demonstrated by refs [2], [10], [11]. In weak magnetic detection, magnetization should be very weak and can be induced by either geomagnetic field or weak permanent magnet. As the steel pipeline itself has original intrinsic magnetization, discontinuities in geometry and material properties near the defects can spontaneously generate weak MFL signals [12], [13], even if there is no stress load or concentration. Such phenomena are potential for passive magnetic detections of pipeline defects [14]–[16]. However, complex random original magnetization may induce a mass of strong interferences to the defect's magnetic features. Therefore, passive weak magnetic detection should be enhanced via reasonable active magnetic excitations.

PMP is a potential lightweight and compact magnetic detection method for pipeline defects via moderate magnetic excitations [4]. Unlike MFLT that uses a pair of large magnets to generate a saturated magnetization, PMP technique utilizes a single small permanent magnet to mildly and locally magnetize the ferromagnetic object and establish a moderate magnetic field throughout all the magnet, gap and test object. A flaw in the object can generate magnetic perturbation signals that are picked up by a coil or magnetometer.

Sun in 2009 wound a coil around a magnet to form a PMP probe [17]. The probe quickly moves over an object containing a defect with a constant lift-off value, and the perturbation signals are picked up by the coaxial coil. This PMP probe array has been adequately developed since 2011 for defect inspections of steel strip, steel rail, thread, coiled tube (outside) and radiator pipe (outside) [18]. The perturbation signal amplitude is proportional to the moving speed of the probe. When PMP probes are implanted onto a PIG for pipeline inspections, intermittent movement with non-constant and low speed will weaken or even disappear the defect signals, or introduce a lot of misleading strong interferences.

A magnetometer instead of the coil can also be used in the PMP probe. Xiao in 2011 placed a Hall sensor below a magnet to form a PMP probe [19]. When tightly touching and scanning the object surface, the probe can clearly image the surface defects in ferromagnetic materials. However, simulation demonstrated that when the lift-off is over 3mm, the difference of the normal magnetic flux density with and without a defect are not obvious. Aguila in 2016 used a Giant Magneto-Resistance (GMR) sensor in the PMP probe to detect and characterize surface cracks in steel plates [20]. It was demonstrated that with the lift-off being zero, peak-to-peak amplitude and interval are capable of characterizing the depth, width, and orientation angle of the crack. However, for the PIG running inside a pipeline, the lift-off value of the probe cannot be zero. In one hand, the pipe inwall has an anti-corrosion coating; in the other hand, the probe will be sealed by a polyurethane layer thicker than 4mm in order to withstand high pressure and severe wear. The lift-off value from the sensor to the pipe inwall cannot be very small.

Taking into account both the compatibility with PIGs and light-weight and low-cost requirements for in-line pipeline inspections, this paper proposes a new defect detection method through compact off-axis local magnetization and sensing by deploying a tiny magnetic sensor below the edge of the magnet. First, the design of the magnetic probe layout is optimized via finite element simulation (FES); Second, the probe's high performances of defect detection, such as signal enhancement, large lift-off, independent of moving speed, and redundancy, repeatability and consistency, are thoroughly demonstrated by various comprehensive experiments; Finally, the capacity of detecting the real OSH is experimentally demonstrated.

II. MAGNETIC PROBE DESIGN

Fig. 1 shows three alternative configurations of the magnetic probe. As shown in Fig. 1 (a), if the magnetic sensor is directly placed below the magnet, the magnetic field will be so large that the sensor will saturate and is unable to perceive

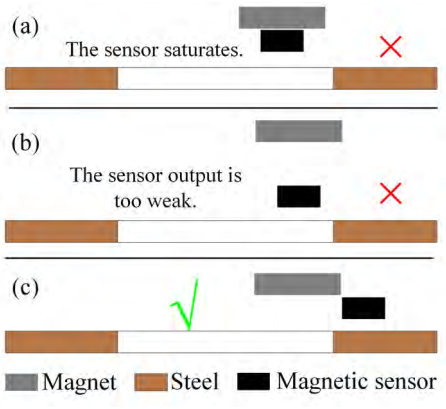

FIGURE 1. Different deployments of magnet and magnetic sensor in the probe.

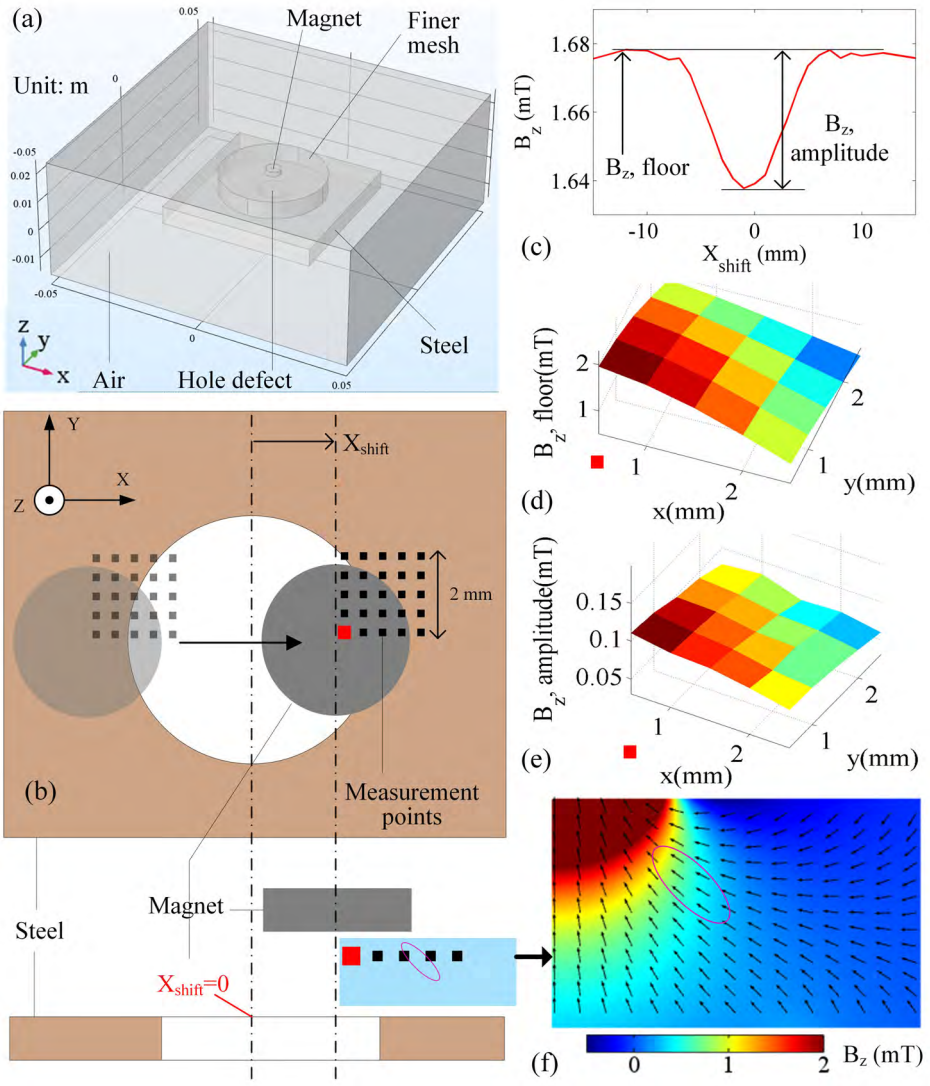

FIGURE 2. Finite element simulations for determining proper position of the magnetic sensor relative to the magnet: (a) simulation model; (b) sweep the position of the probe consisting of a magnet and 5 × 5 measurement points while passing over a hole defect; (c) scan curve of one measurement point; (d) B_z floor measured at the 25 points; (e) B_z amplitude measured at the 25 points; (f) B_z and magnetic vector distributions on one vertical section.

the presence of a defect. As shown in Fig. 1(b), if the distance between the magnetic sensor and the magnet is enlarged, the distance between the magnet and the object to be tested will also increase. In this case, the magnetization to the object will be significantly weakened, and the magnetic anomaly caused by the defect will become very weak and cannot be perceived by the magnetic sensor. As shown in Fig. 1 (c), the proposed scheme uses an off-axis configuration via placing the magnetic sensor below the edge of the magnet. In this case, the magnet can be very close to the object and the magnetizations are therefore sufficient. The magnetic field below the magnet edge is weaker than that below the magnet center, so the magnetic sensor does not saturate. Gradient variances of the magnetic field intensity and direction below the magnet edge are very active; Magnetic field here is very sensitive to changes of the object appearance. Therefore, the magnetic anomaly of the defect detected by this configuration will be more noticeable than that by the other two configurations, and easy to be perceived by the magnetic sensor.

After the magnetization scheme shown in Fig. 1(c) is determined, a finite element simulation (FES) model is built as shown in Fig. 2(a) to find optimal measurement points. A magnet is located above a steel plate with a through hole defect in its center. The magnet and the steel plate are immerged in the air. In order to improve the calculation accuracy, the area between the magnet and the steel plate containing potential measurement points is finely meshed. X_{shift}, the position of the magnet, is parametrically swept so that the magnet moves along the X axis and passes over the hole defect. As shown in Fig. 2(b), 5 × 5 measurement points

with 0.5 mm interval are selected in one corner below the magnet. These measurement points move together with the magnet along the X axis. Taking one measurement point as an example, the curve of the vertical magnetic component B_z as a function of X_{shift} is shown in Fig. 2(c). Fig. 2 (c) also shows the definitions of B_z, *floor* and B_z, *amplitude*.

Fig. 2 (d) and (e) display B_z, *floor* and B_z, *amplitude* of each measurement point. It can be seen that both of them decrease as the measurement point is gradually away from the center of the magnet. This means that if the measurement point is too close to the magnet center, the magnetic sensor may easily saturate and a Hall magnetic sensor with wide measurement range is required. The resolution of the Hall sensor is too low to identify the magnetic anomaly caused by the defect that is much smaller than the background field. If the measurement point is too far away from the magnet center, the magnetic anomaly caused by the defect is too weak due to insufficient magnetizations and will submerge in the noise floor; Even if a highly sensitive magnetoresistive sensor is employed, the defect magnetic anomaly is still difficult to identify.

Fig. 2 (d) and (e) demonstrate that in the area below the magnet edge, both B_z, *floor* and B_z, *amplitude* of the defect-induced magnetic anomaly are moderate; in this area there are good measurement points. Fig. 2 (f) displays the B_z distribution in the baby blue region in Fig. 2(b), and the arrow indicates the magnetic field direction. A pink elliptical circle is located below the edge of the magnet. It can be seen that changes of the magnetic intensity and direction distributed in this area are very noticeable. As the magnetic gradient here is large, the magnetic field in this area is more susceptible to the defect of the steel object. The amplitude of the magnetic anomaly signal detected when the measurement point is selected in this area will be very large. Therefore, the proposed and fabricated magnetic probe deploys the magnetic sensor below the edge of the magnet, as shown in Fig. 3.

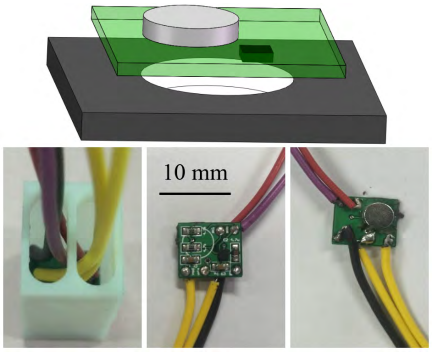

FIGURE 3. Schematic and photos of the designed and fabricated probe.

The plate model can reflect an actual pipe. First, the diameter of the pipe is much larger than the pipe wall thickness, defect size, and magnetic probe size. The pipe locally looks flat enough and very similar to the plate. Second, strong magnetization enhances the magnetic anomaly at the defect, making the difference between the background magnetic fields that are induced by the pipe and the plate themselves insignificant.

Simulations were carried out to compare the difference of the magnetic anomalies of the defects on a plate and a pipe detected via off-axis magnetizations and sensing. The results are shown in Fig. 4. It can be seen that the shapes of the two scanning curves are almost the same except for slight DC offset difference, which confirmed the above claims and the rationality of using flat plate to test the performance of the designed magnetic probe and optimize its configuration. When optimizing the magnetic probe configuration, a large number of scan tests are required for various defects. Testing plate will have consistent results as testing pipe, and the former is more convenient. Therefore, the authors use plate instead of tubular model directly in simulation and experiment.

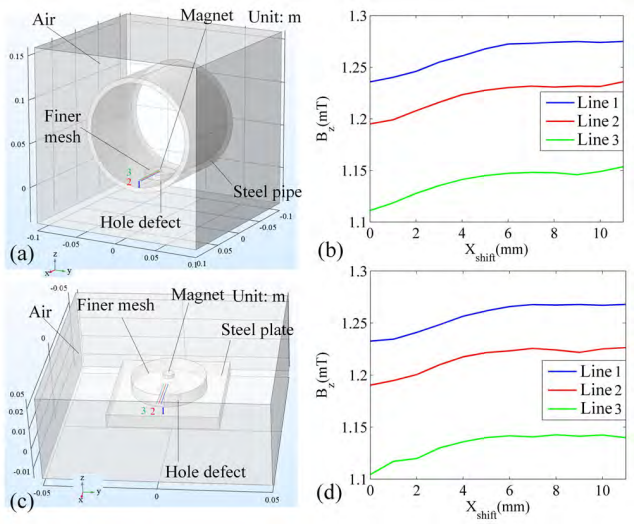

FIGURE 4. Simulation comparisons between pipe (a, b) and plate (c, d) models.

III. PERFORMANCE TEST EXPERIMENTS

Because the probe size ($\sim$ 10 mm) is small enough relative to the pipe diameter (larger than 200 mm), defects on a pipeline can be simulated by defects on a steel plate. Three kinds of defects, through holes, blind holes and slits of different sizes, were manufactured on steel plates, in order to verify the performance of the proposed magnetic probe for detecting steel defects, as shown in Fig. 5. The radius of the through hole and the blind hole is denoted as R, and the width of the slit is denoted as d. Large through hole acts as the OSH. During the test experiment, the probe was manually moved to pass over the defect and triaxial magnetic signals are recorded; magnetic abnormal signals of all kinds of defects were collected. Five sets of validation experiments were carried out: (1) Effect comparisons of measuring the defect magnetic anomaly with and without a magnet; (2) Lift-off range when effective detections were achieved; (3) Influences of different scanning paths on the detected magnetic anomaly

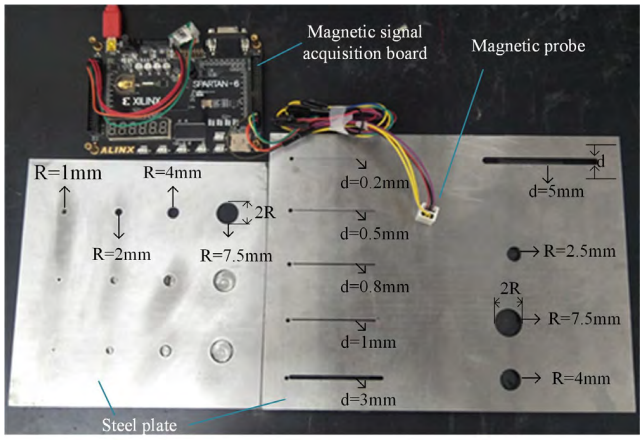

FIGURE 5. Experiment apparatus.

characteristics; (4) Influences of moving speed on detection performances; (5) Redundancy, repeatability and consistency verifications.

IV. RESULTS AND DISCUSSIONS

A. DEFECT'S MAGNETIC CHARACTERISTIC ENHANCEMENTS

Keeping the lift-off value and the probe's scan route unchanged, the normal magnetic signals of the probe while passing over defects were recorded under the magnetization by the geomagnetic field and the magnetization by the proposed scheme, respectively. In order to make a clear comparison between the magnetic characteristics in these two scenarios, the initial values were subtracted from the raw measured magnetic signals. Four representative results are shown in Fig. 6: magnetic anomaly signals of a 0.5 mm wide slit, a hole with radius of 2 mm, a blind hole with radius of 4mm, and an OSH with radius of 5 mm. Parameters that characterize the magnetic anomaly of a defect are defined as shown in Fig. 6 (a). Compared with the passive detection results under the geomagnetic field, the magnetic characteristics of each defect roughly remain unchanged, but the characteristic intensities are significantly enhanced by active magnetizations (AMs), including the difference between the initial and the termination values and the peak-peak amplitude of the defect's magnetic anomaly.

The magnetic anomalies of all the tested defects with different sizes and shapes were measured and their magnitudes are listed in Table 1. It can be seen that the magnetic anomalies of various defects are significantly enhanced by off-axis magnetization and sensing. As for the peak-peak values of the magnetic anomaly, most of them are increased by 2-12 times, and some are increased by more than 20 times. For the floor differences of the magnetic anomaly, all of them are enhanced; half of them are increased by more than 3.5 times, one third are increased by more than 5 times. Therefore, off-axis magnetization and sensing have better detection performances. Enhancements of the defect magnetic anomaly characteristics can bring many benefits for field applications. First, detection missing risk can be lowered as the characteristic signal is not easily submerged in the noise floor. Second, the lift-off value of effective detection can be enlarged, allowing the glue package of the probe to be thick enough to increase wear resistance. Third, smaller defects can be detected with a certain constant lift-off value.

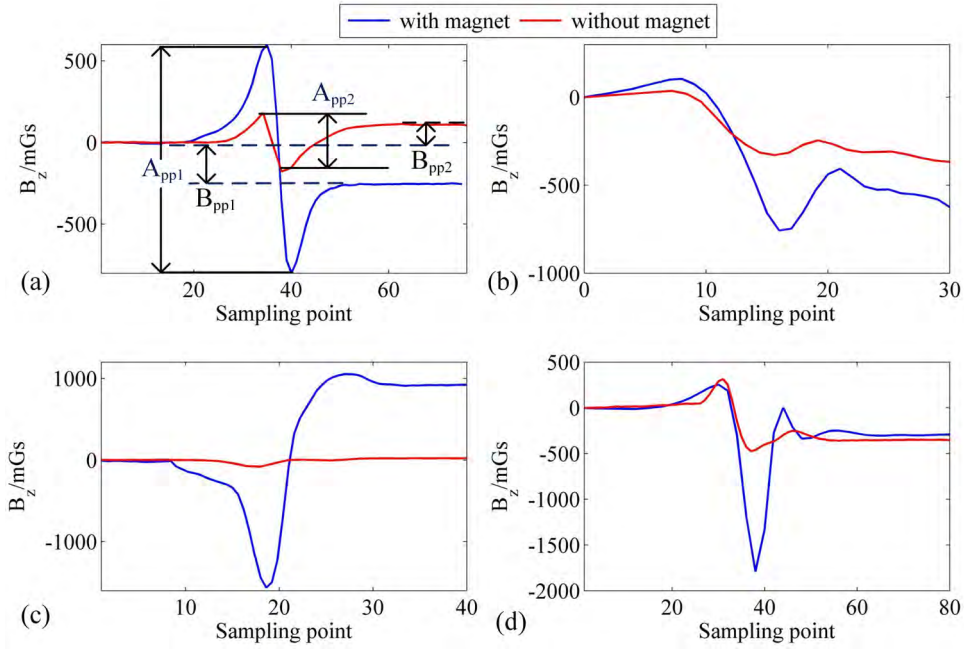

FIGURE 6. Four examples of defect's magnetic signals with and without AMs: (a) 0.5 mm wide slit, (b) hole with radius of 2 mm, (c) blind hole with radius of 4mm, and (d) OSH with radius of 5 mm.

TABLE 1. Magnetic anomaly characteristic comparisons for different defects with and without AMs.

Defect Size (mm)	Hole radius, R				Seam width, d					Blind hole radius, R			
	2	5	7.5	10	0.5	0.8	1	3	5	1	2.5	4	7.5
A_{pp1} (mGs)	342	2628	3878	4104	1365	1698	2410	1556	4012	1279	2131	2592	2340
A_{pp2} (mGs)	180	232	402	389	351	472	403	741	325	253	255	118	198
A_{pp1}/A_{pp2}	1.9	11.3	9.67	10.6	3.89	3.60	5.9	2.10	12.3	5.06	8.36	21.9	11.8
B_{pp1} (mGs)	249	226	744	666	240	290	400	1202	2577	1260	1908	970	1291
B_{pp2} (mGs)	71	127	112	166	107	204	300	624	149	253	341	106	177
B_{pp1}/B_{pp2}	3.5	1.78	6.64	4.01	2.24	1.42	1.33	1.93	17.3	1.56	5.6	9.15	7.29

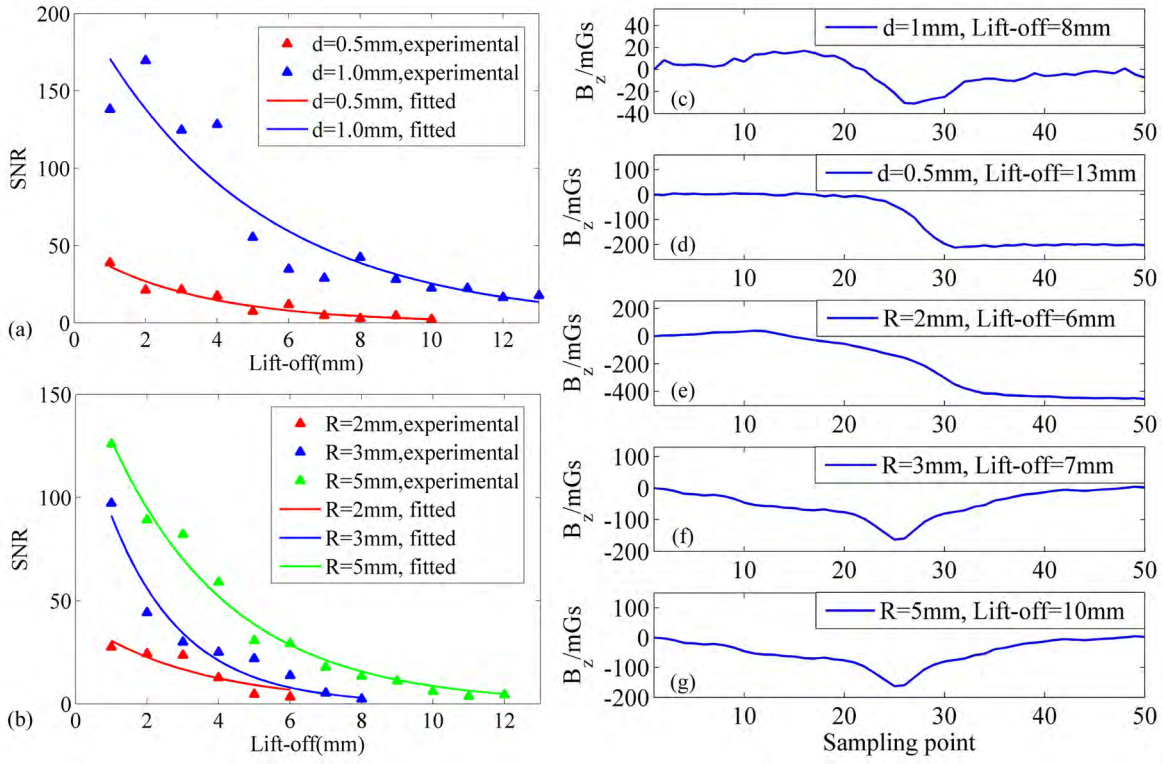

FIGURE 7. SNR with different lift-off values for slit (a) and hole(b) defects; Curve fitting function: $y = ae^{-bx}$.

B. EFFECTIVE LIFT-OFF VALUES

Non-magnetic plastic spacers of different thicknesses are placed between the probe and the steel plate to obtain different lift-off values. Move the probe over a defect and record the magnetic anomaly signals, and then increase the lift-off value and repeat the above process until the signal-to-noise ratio (SNR) approaches zero. The SNR here is defined as the ratio of the peak-to-peak value of the defect's magnetic anomaly to the noise floor of the sensor. Repeat the above procedures for slits of 0.5 mm and 1 mm width, and OSHs with radius of 2 mm, 3 mm, and 5 mm. The experimental results are displayed in Fig. 7 (a) and (b), in which each set of measurement data was fitted according to the equation $y = ae^{-bx}$ [21]. It is worth noting that the largest lift-off values for all the defects are 6 mm $\sim$ 13 mm, which is much larger than those in the literatures [16] (2mm, experimentally demonstrated), [18] (3.3mm, simulation demonstrated), [22] (3.5mm, experimentally demonstrated), [23] (4mm, as close as possible, and [24] (0.3 mm, experimentally demonstrated). For the slits of 0.5 mm and 1 mm width, the largest lift-off values reach 10 mm and 13 mm, respectively; For defects and OSHs with radius of 2mm, 3mm and 5mm, the largest lift-off values reach 6mm, 8mm and 13mm, respectively. Original signal when the liftoff values approach their limits are displayed in Fig. 7 (c)-(g). The SNR decreases as the lift-off value increases. As the radius of the OSH increases, the largest lift-off value increases, and as the slit width increases, the largest lift-off value increases. In order to protect the probe from being damaged by friction and wear, when equipped onto a PIG the outer surface of each probe

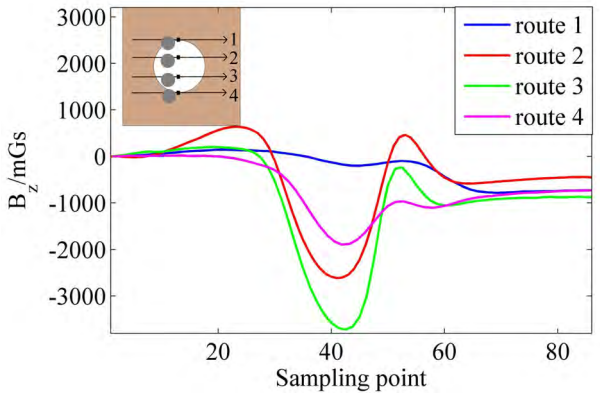

FIGURE 8. Detection results of the probe scanning an OSH along different routes; $R = 10$mm.

need to be adhered with a polyurethane layer thicker than 5 mm. The effective lift-off value for various types of defects has far exceeded that thickness, so the proposed method is especially suitable for the defect detections of a field pipeline based on a PIG.

C. EFFECTS OF SCAN ROUTE

A probe on the PIG may pass over a pipe defect in different directions. To simulate such scenario, the probe was moved along different routes respectively to pass over a hole as shown in Fig. 8, and a slit as shown in Fig. 9. The black square and the grey circle represent the magnetic sensor and the magnet. It can be seen that the moving route of the magnetic sensor is vertically symmetrical about the defect center, but that of the magnet is not, resulting in the magnetization effects of the magnet on the defect along the routes 1, 4 and the routes 2, 3 are not completely identical. B_z on routes 2 and 3 are similar and both of them have a "U" shape, which indicates that the probe can still detect the OSH even if its route does not pass over the defect center. B_z on routes 1 and 4 are much less noticeable than that on routes 2 and 3. This is because the magnetization variance is not large enough when the probe slides along the edge of the defect where both the air and steel domains exist below the probe.

Experiments show that the shape of the magnetic anomaly of the slit defect is independent of the scanning route, as shown in Fig. 9. In Fig. 9(a), the angles between the scan routes and the slit are about 45 degrees; while in Fig. 9 (b), the scan routes are perpendicular to the slit. In the two scenarios, the measured eight curves are almost identical with regards to both the amplitude and the shape. Comparing the curves in the two scenarios, the widths of the magnetic characteristics are a little different for different scanning direction because the distance across the slit is not the same.

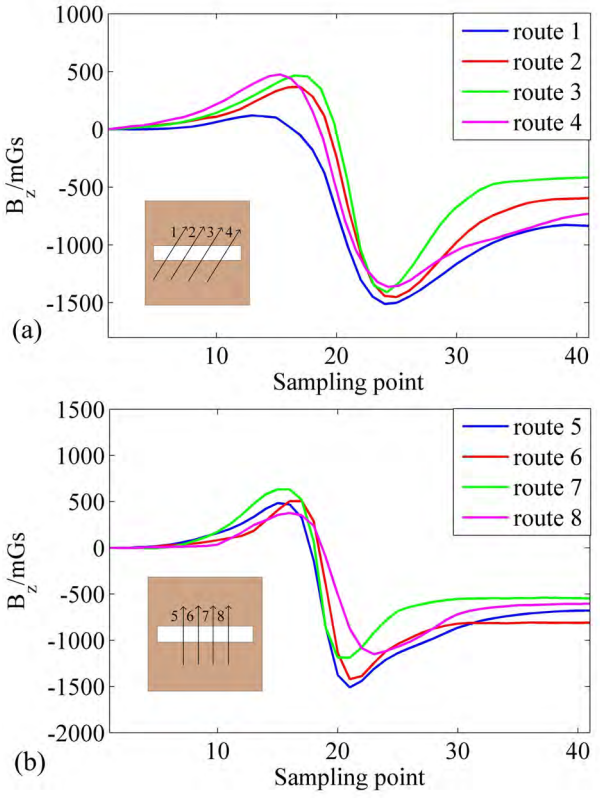

FIGURE 9. Detection results of the probe scanning a slit defect along different routes; $d = 0.5$mm.

D. INDEPENDENCE OF SCAN SPEED

The speed of the pressure-difference-driven PIG is not constant due to pressure fluctuations and randomly varying friction. Defect detection technologies based on PMP require high and stable moving speed as a pick-up coil that winds around the permanent magnet is used, so they are not suitable for pipeline defect detection. Instead, the performance of the proposed probe is independent of moving speed. Magnetic signals of OSHs with $R = 5$mm and 10mm at different scanning speeds were measured. The results are displayed in Fig. 10. It can be seen that the probe can always clearly detect the OSHs at three different speeds of about 1 m/s, 0.25 m/s and 0.05 m/s. Both the amplitude and shape of the magnetic characteristics are almost identical. Therefore, the proposed magnetic probe can detect clear and stable

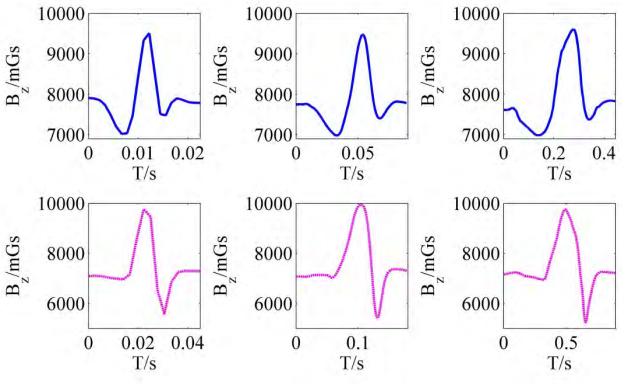

FIGURE 10. Magnetic signals when the probe passes over OSHs with $R = 5$mm (upper row) and 10mm (lower row) at different speeds.

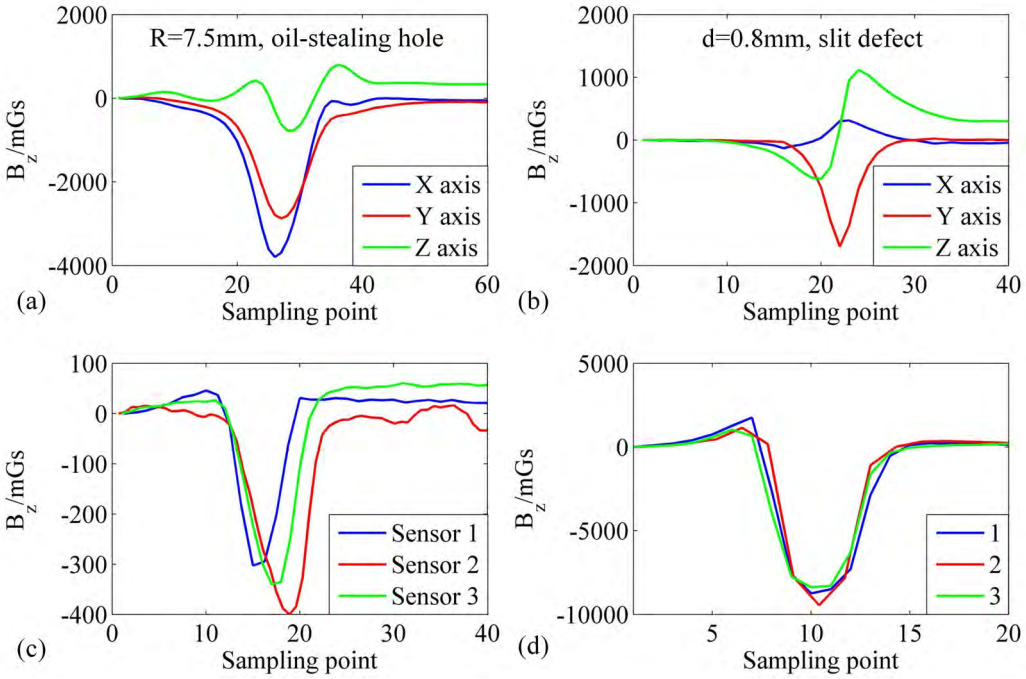

FIGURE 11. Redundancy (a) and (b), consistency (c), and repeatability (d) of the proposed probe.

defect signals at different speeds, which is very favorable for being implemented onto a PIG.

E. REDUNDANCY, CONSISTENCY, AND REPEATABILITY

The proposed probe employs triaxial magnetoresistive sensor, which is much smaller and lighter than magnetic fluxgate sensor, and has much higher sensitivity than magnetic Hall sensor. Triaxial sensing capacity may be redundant for detecting a defect, but can contribute to lowering the detection-missing risk. In some cases, due to the residual stress and magnetization, the response characteristics of a defect to magnetizations may deviate from most defects, resulting in that B_z characteristic is vague and inconspicuous. It is necessary to use the other two tangential components to indicate the defect.

Fig. 11 (a) displays triaxial magnetic characteristics of an OSH with $R = 7.5$ mm. It can be seen that the normal component B_z is not as noticeable as the tangential components; If B_z is used alone for defect detection, the hole may be missed. Fig. 11 (b) displays triaxial magnetic characteristics of a slit with $d = 0.8$ mm. Both B_z and B_y noticeably indicate the slit defect. Therefore, the use of triaxial magnetic detection can increase the redundancy and reduce the detection-missing rate.

In addition, both the consistency of the probe and the repeatability of the defect detection are very good. Fig. 11 (c) displays the magnetic signals of one OSH with $R = 6$mm measured by three probes. It can be seen that the magnetic characteristics have similar shape and amplitude except for some little biases that do not hinder defect identification. Fig.11 (d) shows the magnetic signals of one blind hole with $R = 6$mm scanned by one probe for three times. It can be seen that the measured curves almost completely overlap.

V. APPLICATION IN OSH AND SMALL DEFECT DETECTION

On one section of steel pipe with the diameter of 6 inches, an OSH with an inner radius of 10 mm was machined, and then an oil-stealing branch pipe with the same inner diameter was welded onto the hole, as shown in Fig. 12(a). A cylindrical internal detector was fabricated by using 3D printing technology, as shown in Fig. 12(b). Magnetic probes are installed in the grooves of the inner detector. The distance between adjacent probes is 16.2 mm. One push rod was used in the experiment to control the movement of the inner detector inside the pipe, as shown in Fig. 12(a) and (c). In the field pipeline inspection, the cylindrical detector can always closely contact with the pipe wall like a piston via two polyurethane bowls. As the fluid pressure is uniform on the polyurethane bowl, the inner detector is completely axially driven, and the detector axis can always keep parallel with the pipeline axis to achieve stable constant liftoff value between the circularly distributed magnetic probes and the pipe wall. In order to mimic such a field running condition, a guide cover for restraining the push rod was designed and installed at one end of the pipe so that the inner detector is always axially driven, as shown in Fig. 12(a).

The distribution of the magnetic probes is shown in Fig. 12(d). Double rows of probe array are employed. Magnetic probes in the two rows are shifted by a certain angle

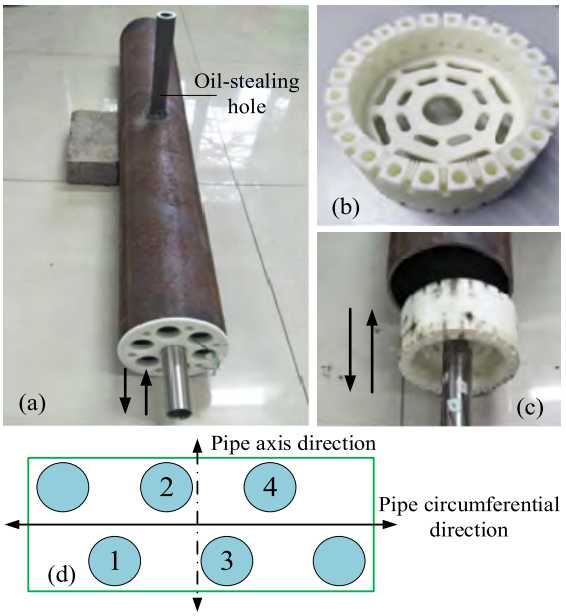

FIGURE 12. OSH detection experiment and probe layout.

to increase the density of the scan lines. The OSH in Fig. 12(a) can be completely cover by four magnetic probes. For smaller holes, the number of rows of magnetic probes needs to be increased and the shift angle of the array elements in adjacent rows needs to be decreased in order to further increase the scan line density. As the inner detector moves inside the pipe, the probes No. 2 and No. 4 pass over the OSH at the same time first; the probes No. 1 and No. 3 pass later. The test results are shown in Fig. 13. Both No. 2 and No. 3 probes detect a ''U'' shaped magnetic anomaly signal. Because the axial positions of these two probes are different, as shown in Fig. 12(d), the moments when the two magnetic anomaly signals appear are slightly different. These two signals clearly indicate the presence of the OSH. The magnetic anomaly signals are also detected by the No. 1 and No. 4 probes, but are less noticeable than that by Nos 2 and 3. According to the steel plate experiment results shown in Fig. 8, these magnetic abnormal signals correspond to the outer edge of the OSH.

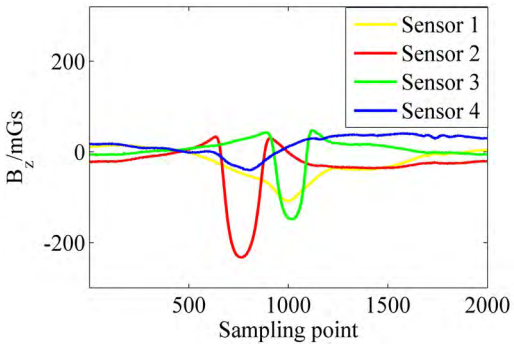

FIGURE 13. OSH detection results.

In order to demonstrate that the system can detect the corrosion pits like ref. [9], the author manufactured some small blind holes on the inner wall of a steel pipe via electric discharge machining. The blind holes represent corrosion pits. Through holes that are much smaller than OSH were also manufactured on the steel pipe. The proposed system is used to scan these small blind and through holes and detect their magnetic anomalies. The results are shown in Fig. 14. It can be seen that all of them are detectable by this method, just like that those similar defects on a steel plate are detectable. The capacity of detecting corrosion pits and small defects are demonstrated.

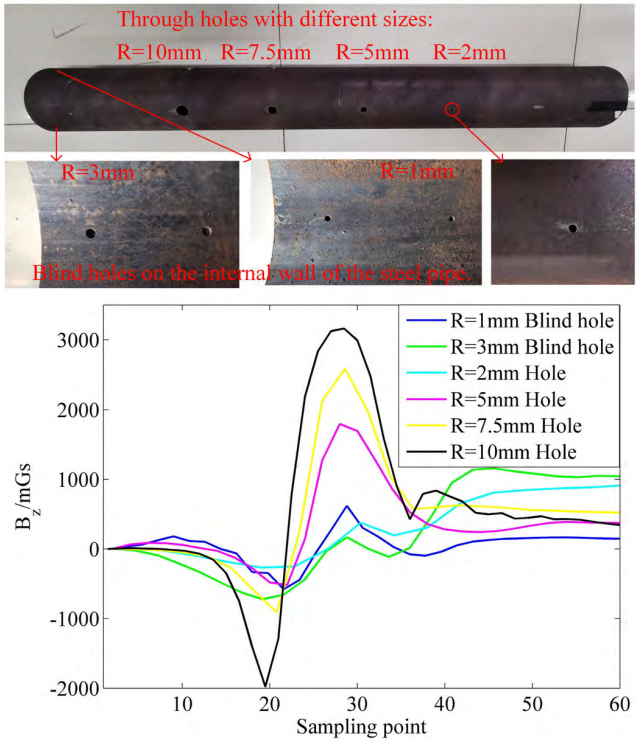

FIGURE 14. Small defect detection results for a steel pipe.

VI. CONCLUSIONS

This paper demonstrates a new lightweight, high performance detection method of pipeline defects through compact off-axis magnetization and sensing. The proposed magnetic probe uses a small magnet to locally magnetize the object to be tested, and deploys a tiny magnetoresistive sensor below the edge of the magnet instead of below its center to sense the magnetic anomaly caused by the defect. FESs demonstrate that such configurations can prevent the magnetic sensor from saturation while maintaining high magnetic sensitivity of defect detections.

Experiments demonstrate that the sensitivity of the proposed scheme is mostly 2-12 times that of passive magnetic detection without AMs; in some cases, up to 20 times. The effective lift-off values are as high as 6mm-13mm, which exceeds conventional magnetic detection methods and is also much larger than the thickness of the protective polyurethane layer on the probe required by field pipeline detector. In addition, triaxial detection capacity of the probe can greatly reduce the risk of missed detection; the defect magnetic

signature detected is independent of moving speed and is therefore ideal for the in-pipe detector with unstable running speeds. The ability to detect the real OSH is experimentally demonstrated.

REFERENCES

[1] H. R. Vanaei, A. Eslami, and A. Egbewande, "A review on pipeline corrosion, in-line inspection (ILI), and corrosion growth rate models," *Int. J. Pressure Vessels Piping*, vol. 149, pp. 43–54, Jan. 2017.

[2] X. Sun and B. Liu, "Weak magnetic detection for stolen oil hole on long-distance transportation pipeline," *J. Shenyang Univ. Technol.*, vol. 36, no. 4, pp. 436–440, Jul. 2014.

[3] W. L. Shao, J. Z. Chen, and Y. L. Ma, "The recognition of in-line inspection magnetic flux leakage signals of oil-stealing pipeline hole," *Nondestruct. Test.*, vol. 39, no. 5, pp. 6–9, 2017.

[4] S. Liu, Y. Sun, M. Gu, C. Liu, L. He, and Y. Kang, "Review and analysis of three representative electromagnetic NDT methods," *Insight-Non-Destructive Test. Condition Monit.*, vol. 59, no. 4, pp. 176–183, 2017.

[5] Y. Zhang, M. Zheng, C. An, J. K. Seo, I. P. Pasqualino, F. Lim, and M. Duan, "A review of the integrity management of subsea production systems: Inspection and monitoring methods," *Ships Offshore Struct.*, to be published. doi: 10.1080/17445302.2019.1565071.

[6] Y. Shi, C. Zhang, R. Li, M. Cai, and G. Jia, "Theory and application of magnetic flux leakage pipeline detection," *Sensors*, vol. 15, no. 12, pp. 31036–31055, Dec. 2015.

[7] Q. Feng, R. Li, B. Nie, S. Liu, L. Zhang, and H. Zhang, "Literature review: Theory and application of in-line inspection technologies for oil and gas pipeline girth weld defection," *Sensors*, vol. 17, p. 50, Jan. 2017.

[8] J. Quarini and S. Shire, "A review of fluid-driven pipeline pigs and their applications," *J. Process Mech. Eng.*, vol. 221, pp. 1–10, Feb. 2007.

[9] Y. He, G. Y. Tian, H. Zhang, M. Alamin, A. Simm, and P. Jackson, "Steel corrosion characterization using pulsed eddy current systems," *IEEE Sensors J.*, vol. 12, no. 6, pp. 2113–2120, Jun. 2012.

[10] M. Yilai and L. Li, "Research on internal and external defect identification of drill pipe based on weak magnetic inspection," *Insight-Non-Destructive Test. Condition Monit.*, vol. 56, no. 1, pp. 31–34, 2014.

[11] B. Liu, Y. Cao, H. Zhang, Y. R. Lin, W. R. Sun, and B. Xu, "Weak magnetic flux leakage: A possible method for studying pipeline defects located either inside or outside the structures," *NDT E Int.*, vol. 74, pp. 81–86, Sep. 2015.

[12] Z. C. Qian, H. H. Huang, G. Han, B. Xiong, Z. Y. Fei, and L. W. Zhao, "Review on metal magnetic memory detection technology in remanufacturing and case study in engineering," *J. Mech. Eng.*, vol. 54, no. 17, pp. 235–245, Sep. 2018.

[13] S. Bao, M. Fu, S. Hu, Y. Gu, and H. Lou, "A review of the metal magnetic memory technique," in *Proc. Int. Conf. Offshore Mech. Arct. Eng. (OMAE)*, vol. 4, 2016, Art. no. V004T03A006.

[14] Y. Li, X. Zeng, L. Wei, and Q. Wan, "Characterizations of damage-induced magnetization for X80 pipeline steel by metal magnetic memory testing," *Int. J. Appl. Electromagn. Mech.*, vol. 54, no. 1, pp. 23–35, Apr. 2017.

[15] B. Liu, Z. Ma, L. He, D. Wang, H. Zhang, and J. Ren, "Quantitative study on the propagation characteristics of MMM signal for stress internal detection of long distance oil and gas pipeline," *NDT E Int.*, vol. 100, pp. 40–47, Dec. 2018.

[16] B. Liu, L. He, Z. Ma, H. Zhang, S. Sfarra, H. Fernandes, and S. Perilli, "Study on internal stress damage detection in long-distance oil and gas pipelines via weak magnetic method," *ISA Trans.*, vol. 89, pp. 272–280, Jun. 2019.

[17] Y. Sun, Y. Kang, and C. Qiu, "A permanent magnetic perturbation testing sensor," *Sens. Actuators A, Phys.*, vol. 155, no. 2, pp. 226–232, Oct. 2009.

[18] Y. Sun, Y. Kang, and C. Qiu, "A new NDT method based on permanent magnetic field perturbation," *NDT E Int.*, vol. 44, no. 1, pp. 1–7, Jan. 2011.

[19] C. Xiao and Y. Zhang, "A method of magnetic scanning imaging for detecting defects in ferromagnetic materials," *Meas. Sci. Technol.*, vol. 22, no. 2, Feb. 2011, Art. no. 025503.

[20] J. Aguila-Muñoz, J. H. Espina-Hernández, J. A. Pérez-Benítez, F. Caleyo, and J. M. Hallen, "A magnetic perturbation GMR-based probe for the nondestructive evaluation of surface cracks in ferromagnetic steels," *NDT E Int.*, vol. 79, pp. 132–141, Apr. 2016.

[21] H. Q. Pham, B. V. Tran, D. T. Doan, V. S. Le, Q. N. Pham, K. Kim, C. Kim, K. Kim, F. Terki, and Q. H. Tran, "Highly sensitive planar Hall magnetoresistive sensor for magnetic flux leakage pipeline inspection," *IEEE Trans. Magn.*, vol. 54, no. 6, Jun. 2018, Art. no. 6201105.

[22] L. Peng, S. Huang, S. Wang, and W. Zhao, "A lift-off revision method for magnetic flux leakage measurement signal," in *Proc. I2MTC*, Piscataway, NJ, USA, 2018, pp. 1–5.

[23] P. Li, G. J. Zhou, C. W. Wang, B. Zhou, and X. B. Wang, "New method of axis orbit detection based on permanent magnet perturbation sensor," *Sensors Microsyst.*, vol. 38, no. 4, pp. 30–32, Apr. 2019.

[24] Z. Cai, S. Liu, C. Zhang, L. Jin, and Q. Yang, "Finite element analysis and optimum design of permanent magnetic field perturbation testing," *J. Elect. Technol.*, vol. 30, no. 3, pp. 67–72, Feb. 2015.

LI JIAN received the B.E., M.E., and Ph.D. degrees from TJU, in 1994, 1997, and 2000, respectively, where he is currently a Professor. His research interests include pipeline leak detection and pipeline safety warning.

GE YU received the B.S. degree from the Shandong University of Automation, in 2018. She is currently pursuing the master's degree with the Instrument Science and Technology Department, Tianjin University. Her research interests include defect detection of pipelines.

HUANG XINJING received the B.S. and Ph.D. degrees from TJU, in 2010 and 2016, respectively, where he is currently an Assistant Professor. His research interest includes pipeline damage detections.